Proceedings of the ASME 2015 International Design Engineering Technical Conferences & Computers and Information in Engineering Conference
IDETC/CIE 2015
August 2-5, 2015, Boston, USA

DETC2015/46106

ISOLATED RESPONSE CURVES IN A BASE-EXCITED, TWO-DEGREE-OF-FREEDOM, NONLINEAR SYSTEM

J.P. Noël*, T. Detroux, L. Masset, G. Kerschen

Space Structures and Systems Laboratory
Aerospace and Mechanical Engineering Department
University of Liège
Liège, Belgium

L.N. Virgin

Nonlinear Dynamics Group
School of Engineering
Duke University
Durham, North Carolina, USA

ABSTRACT

In the present paper, isolated response curves in a nonlinear system consisting of two masses sliding on a horizontal guide are examined. Transverse springs are attached to one mass to provide the nonlinear restoring force, and a harmonic motion of the complete system is imposed by prescribing the displacement of their supports. Numerical simulations are carried out to study the conditions of existence of isolated solutions, their bifurcations, their merging with the main response branch and their basins of attraction. This is achieved using tools including nonlinear normal modes, energy balance, harmonic balance-based continuation and bifurcation tracking, and global analysis.

1 INTRODUCTION

Isolated response curves (usually abridged as *isolas*) are an intriguing feature of nonlinear dynamics. They correspond to closed loops of solutions emerging in nonlinear frequency responses and which are, by definition, detached from the main response branch [1]. Isolas may thus go easily undetected in the analysis of the forced response of a nonlinear system, whether it be numerically employing classical continuation techniques, or experimentally applying sine-sweep excitations. However, an increase in forcing amplitude may cause the merging of the main branch and the isola, resulting in dramatic frequency and amplitude shifts of the resonance location. This renders isolas potentially dangerous in practice for engineers designing systems likely to operate in nonlinear regimes of motion [2, 3].

The present paper constitutes an attempt to the understanding of intrinsic features of isolas, in particular their creation mechanism, the evolution of their bifurcations according to parameter variations, and their probability of realisation. To this end, numerical simulations are carried out on a simple, base-excited mechanical system with nonlinear hardening springs, inspired by the work in Refs. [4, 5]. As it is conjectured that interactions between nonlinear modes underlie the existence of isolas [6], a multi-degree-of-freedom (multi-DOF) system, namely comprising two DOFs, is considered, as described in Section 2. Sections 3.1 and 3.2 analyse in detail the nonlinear modes of the system using an energy balance technique. This yields important insights into the creation of isolas directly based on the undamped, unforced system behaviour. The forced response is also studied in Sections 3.3 and 3.4, where the tracking of limit-point bifurcations versus the amplitude and frequency of excitation is achieved by means of the harmonic balance method. It is revealed that the merging phenomenon occurs through the annihilation of two limit points. Finally, a global analysis of the system provides in Section 3.5 the basins of attraction of isolated solutions. Conclusions of the paper are summarised in Section 4.

*Address all correspondence to this author, email: jp.noel@ulg.ac.be.

2 A BASE-EXCITED, TWO-DEGREE-OF-FREEDOM SYSTEM WITH HARDENING SPRINGS

The system of interest consists of two masses connected through a linear spring and sliding on a horizontal guide, as shown in Fig. 1. The physical and linear modal parameters of the system are listed in Tables 1 and 2, respectively. Two linear but transverse springs are also attached to mass 1, providing a nonlinear restoring force in the horizontal direction. The displacement of the transverse spring supports is prescribed to impart motion to the two masses. The mass and linear stiffness coefficients m_1, m_2, k_1 and k_2 are such that a ratio between the linear natural frequencies of the system of 4.64, that is larger than 3 but slightly smaller than 5, is achieved, as motivated in Section 3.1. Moderate linear damping is finally introduced equally on the two vibration modes.

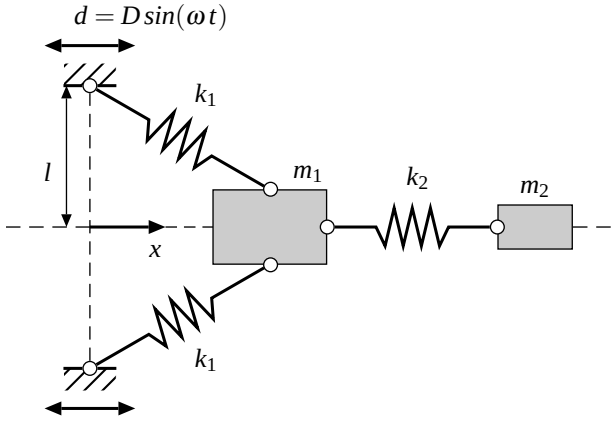

FIGURE 1: Base-excited, 2-DOF system with transverse springs providing a restoring force with hardening characteristic.

$m_1\ (kg)$	$m_2\ (kg)$	$k_1\ (N/m)$	$k_2\ (N/m)$
1	0.2	60	35
$l\ (m)$	$\lambda\ (-)$	$c_1\ (Ns/m)$	$c_2\ (Ns/m)$
0.1	0.9	0.25	0.15

TABLE 1: Physical parameters of the 2-DOF system.

	Natural frequency (Hz)	Damping ratio (%)
Mode 1	0.50	3.25
Mode 2	2.32	3.25

TABLE 2: Linear modal parameters of the 2-DOF system.

The equations of motion of the system in Fig. 1 can be derived by noting that the horizontal projection of the restoring force associated with one of the transverse springs is given by

$$F_x = F\,cos(\theta) = k_1\left(\sqrt{x_1^2+l^2}-l_0\right)\frac{x_1}{\sqrt{x_1^2+l^2}}, \qquad (1)$$

where F is the restoring force in the direction of the spring, θ is the angle between this direction and the horizontal, x_1 is the displacement of mass 1 relative to the displacement of the spring support, l_0 is the undeformed length of the spring and l is its deformed length when mass 1 is at position $x_1 = 0$. Assuming a sinusoidal base excitation applied simultaneously to the supports of the two transverse springs, the equations of motion write

$$\begin{aligned} &m_1\ddot{x}_1 + c_1\dot{x}_1 + c_2\,(\dot{x}_1-\dot{x}_2) + 2k_1\left(1-\frac{\lambda}{\sqrt{1+(x_1/l)^2}}\right)x_1 \\ &\quad + k_2\,(x_1-x_2) = m_1\omega^2 D\,sin(\omega t) \\ &m_2\ddot{x}_2 + c_2\,(\dot{x}_2-\dot{x}_1) + k_2\,(x_2-x_1) = 0, \end{aligned} \qquad (2)$$

where $\lambda = l_0/l$, and where x_2 is the absolute displacement of mass 2, c_1 and c_2 are linear damping coefficients, D is the base displacement amplitude, and ω is the excitation frequency. The nonlinear force term in Eqs. (2) is depicted over a realistic displacement range in Fig. 2 (solid line). The plot also shows Taylor approximations of the third, fifth and seventh order, which all fail to capture the behaviour of the exact curve for large amplitudes of motion. The complete nonlinear expression of the force will thus be considered throughout the study.

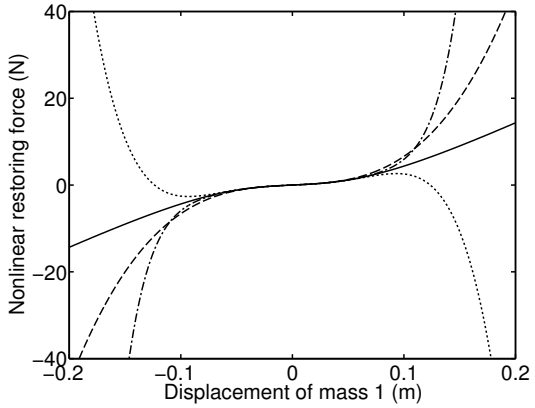

FIGURE 2: Nonlinear restoring force of the 2-DOF system. Exact expression (solid); 3-order (dashed), 5-order (dotted) and 7-order (dash-dotted) Taylor approximations.

3 STUDY OF INTRINSIC FEATURES OF ISOLAS

3.1 Periodic motion of the undamped system: nonlinear normal mode

The concept of normal modes was generalised to nonlinear systems by Rosenberg in the 1960s [7,8] and by Shaw and Pierre in the 1990s [9]. In the present work, an extension of Rosenberg's definition of a nonlinear normal mode (NNM) is considered [10]. Specifically, a NNM of a *n*-DOF nonlinear system is defined as a periodic solution of the undamped and unforced equations of motion

$$\mathbf{M}\,\ddot{\mathbf{q}}(t)+\mathbf{K}\,\mathbf{q}(t)+\mathbf{f}(\mathbf{q}(t))=0, \tag{3}$$

where $\mathbf{M}\in\mathbb{R}^{n\times n}$ is the mass matrix, $\mathbf{K}\in\mathbb{R}^{n\times n}$ is the linear stiffness matrix, $\mathbf{q}(t)\in\mathbb{R}^n$ is the vector of generalised displacements, and $\mathbf{f}\in\mathbb{R}^n$ is the nonlinear restoring force vector. This definition may appear to be restrictive as one focuses herein on isolas in the forced response of a damped system. However, as it will be shown in Section 3.2, the topology of undamped NNMs may yield considerable insights into the creation mechanism of isolas. From a numerical point of view, one calculates NNMs by means of the two-step algorithm proposed in Ref. [11], which combines shooting with pseudo arc-length continuation to find the periodic solutions of Eq. (3). The depiction of the calculated branches of solutions is conveniently achieved in a frequency-energy plot (FEP), where a NNM is a point associated with the frequency of the periodic motion, and with the total conserved energy accompanying the motion.

The FEPs of the two fundamental NNMs of the system in Fig. 1 are displayed in Fig. 3 (a – b). Frequency increases with energy in the two plots, revealing the hardening characteristic of the transverse springs in the system. The topology of NNM 1 is more complicated as it features a loop along the main backbone curve, clearly visible in the inset close-up. This loop, termed α-loop because of its resemblance to the Greek letter, is the symptom of a 3:1 interaction between NNMs, or internal resonance. The dashed line in Fig. 3 (a) represents the FEP of NNM 2 when dividing its frequency by 3. It intersects NNM 1 around 0.8 *Hz*, *i.e.* in the vicinity of the α-loop, causing the modes to interact. This interaction underlies an exchange of energy between modes, visible in the time evolution of the linear modal coordinates depicted at four specific frequency-energy locations along the α-loop in Fig. 3 (A,B,C,D). In particular at points (B) and (C), the significant amplitude of the second modal coordinate, oscillating at a frequency 3 times that of the first modal coordinate, confirms the existence of the 3:1 internal resonance. Note that no 5:1 interaction loop emanates from the NNM 1 backbone, since the FEP of NNM 2 considering one fifth of the frequency, plotted as a dash-dotted line in Fig. 3 (a), lies underneath NNM 1. This was intentionally achieved by setting the ratio of the linear frequencies of the system below 5 in Section 2. This, in turn, implies that a single isola subtended by a α-loop topology exists in the system dynamics, as discussed in the later sections.

3.2 Base displacement amplitude required to obtain nonlinear normal mode motion

NNMs are known to form the backbone of damped frequency response curves calculated at varying force amplitudes [10]. Formally, a damped system driven harmonically vibrates according to an undamped NNM denoted $\mathbf{x}(t)\in\mathbb{R}^n$, and so undergoes phase resonance [12, 13], if the energy dissipated by damping forces over one cycle E_{out} balances the energy provided by the external force E_{in}. Denoting $\mathbf{C}\in\mathbb{R}^{n\times n}$ the linear damping matrix of the system and $\mathbf{p}(t)=A\,e^{i\,\omega\,t}\,\mathbf{e_j}\in\mathbb{R}^n$ a single-point, harmonic forcing applied to DOF j with amplitude A, this translates mathematically into

$$E_{in}=A\int_0^T e^{i\,\omega\,t}\,\dot{\mathbf{x}}^{\mathrm{T}}(t)\,\mathbf{e_j}\,dt=\int_0^T \dot{\mathbf{x}}^{\mathrm{T}}(t)\,\mathbf{C}\,\dot{\mathbf{x}}(t)\,dt=E_{out}, \tag{4}$$

where T is the cycle period, and T is the transpose operation. The relationship in Eq. (4) is essentially approximate since a multiharmonic, multipoint excitation is theoretically needed to initiate a NNM motion [12]. The practical implications of Eq. (4) are however very important. It establishes a direct link between the undamped, unforced system response, and forced resonance conditions. Specifically, it allows to calculate the amplitude A driving the system to resonance, based only on an undamped NNM motion $\mathbf{x}(t)$, as analysed in Section 3.1, and the knowledge of the damping matrix $\mathbf{C}$.

Fig. 4 compares the FEP of NNM 1 in (a) with the base displacement amplitude required to initiate a vibration of the damped system along this NNM in (b), and calculated using Eq. (4). The latter curve exhibits a topology similar to the undamped FEP, including a nonmonotonic increase of amplitude versus frequency (see the inset close-up). As a result, multiple resonance frequencies exist for forcing amplitudes exceeding 5.2 *mm*. For instance, the three black dots in Fig. 4 (b) indicate that the system may resonate at 0.76, 0.81, and 1.08 *Hz* for a base displacement of 7 *mm*. Section 3.4 will demonstrate that 5.2 *mm* (blue dot) is the minimum forcing amplitude responsible for the creation of an isola, and that the resonance points at frequencies of 0.81 *Hz* and 1.08 *Hz* for a 7 *mm* excitation are located on this isola. The key result of the present section is to relate, via an energy balance equation, the existence of modal interactions in an undamped NNM, appearing as α-loop topology features, to the creation of isolas in the forced frequency response.

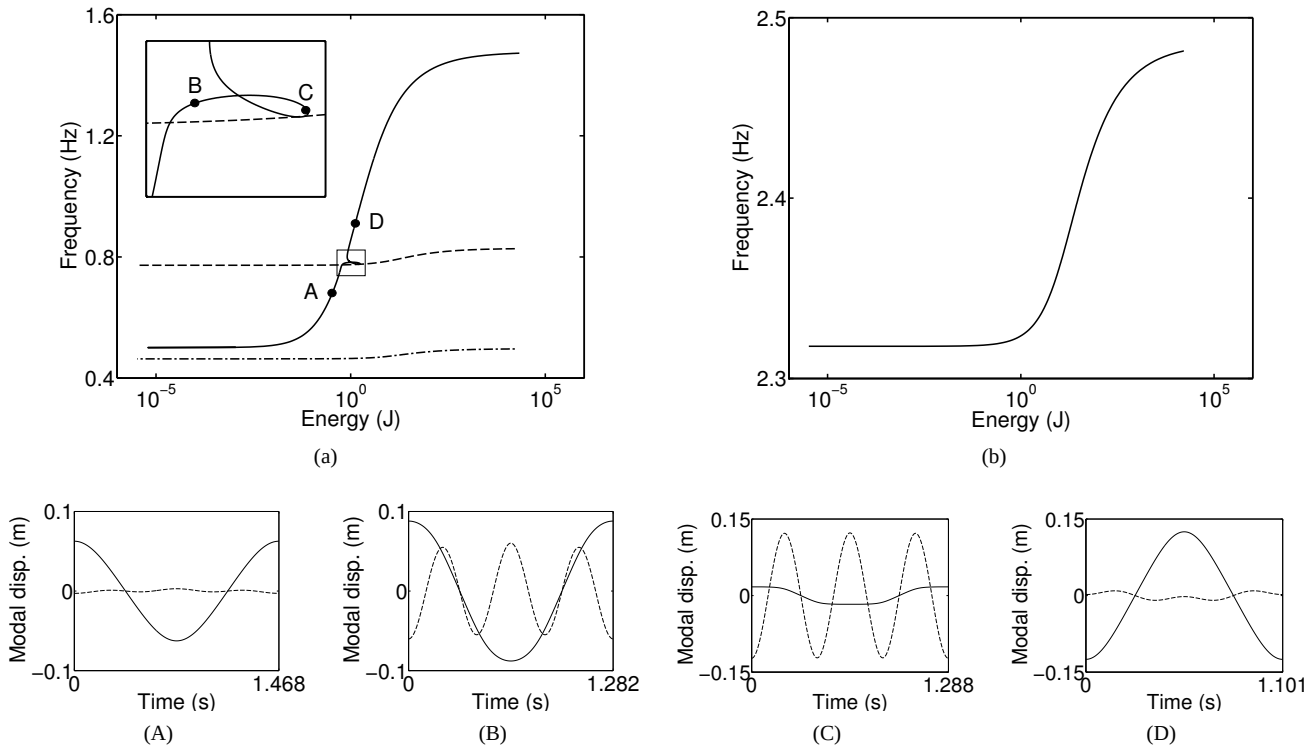

FIGURE 3: FEPs of the (a) first and (b) second NNM of the 2-DOF system. The dashed and dash-dotted lines in (a) represent the FEP of the second NNM when dividing its frequency by 3 and 5, respectively. (A – D) Periodic time evolution of the first (solid line) and second (dashed line) linear modal coordinates of the system plotted at the frequency-energy locations labelled A, B, C, D in (a).

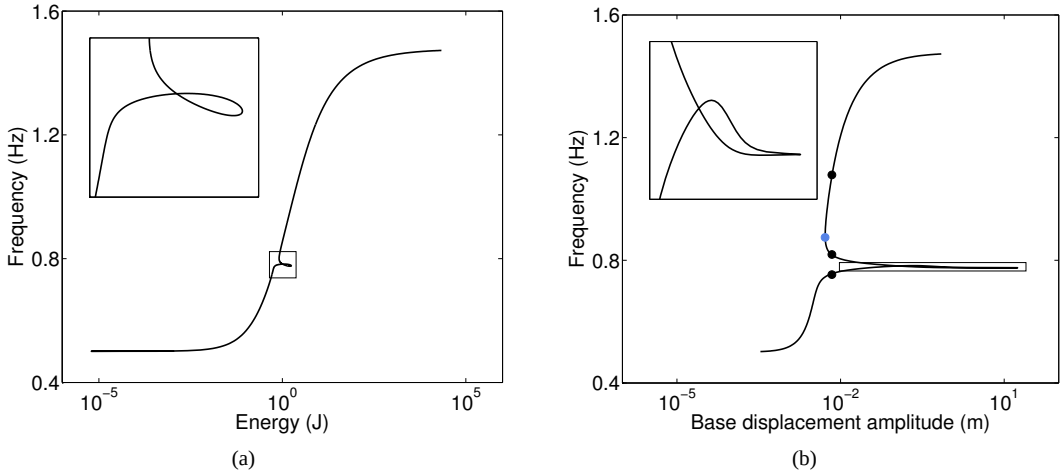

FIGURE 4: (a) First NNM of the undamped, unforced system; (b) amplitude of the base displacement required to initiate a vibration of the damped system along its first NNM. Inset close-ups provide details of the behaviour of the system close to the 3:1 internal resonance.

3.3 Periodic motion of the damped system: nonlinear forced response

The forced behaviour of the system in the case of harmonic base excitations is now studied. Fig. 5 presents the displacement of mass 1 in response to swept-sine forcing profiles of increasing amplitudes, namely 6, 7, 8 and 9 *mm*, and obtained using direct Newmark time integration considering a sweep rate of 1 Hz/min. At each force level, the response time series exhibits a textbook amplitude jump coinciding with the resonance location. Much less documented in the technical literature is the dramatic modification of the resonance frequency from 0.77 to 1.14 *Hz*, that is a nearly 50 % rise, when increasing the forcing amplitude from 7 to 8 *mm*. This frequency jump phenomenon, which will later be attributed to the merging of the main response branch with a 3:1 isola, also implies a potentially dangerous increase of the response amplitude from 0.08 to 0.21 *m*.

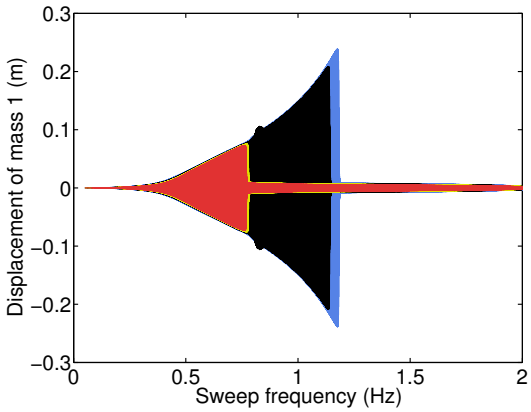

FIGURE 5: Response at mass 1 of the 2-DOF system to a base, swept-sine excitation of increasing amplitude: 6 *mm* (red); 7 *mm* (yellow); 8 *mm* (black); 9 *mm* (blue).

One finally notices in Fig. 5 a brief modulation, occurring around 0.82 *Hz*, of the response envelope observed for a 8 *mm* forcing. This behaviour is further investigated in Fig. 6, where a stepped-sine response computed using harmonic balance-based continuation (in blue) [14] is superposed on the swept-sine time histories. Limit-point (LP) and Neimark-Sacker (NS) bifurcations [15] are indicated on the continuation branch via yellow and red circles, respectively. The inset close-up clearly shows that a NS bifurcation is responsible for the envelope modulation by creating a stable branch of quasiperiodic oscillations, not represented in the figure. A second NS bifurcation transforms the quasiperiodic motion back into stable periodic oscillations. The delay between the two bifurcation points and the exact onset and disappearance of quasiperiodicity in the response is attributed to the transient effects inherent to sine sweeps.

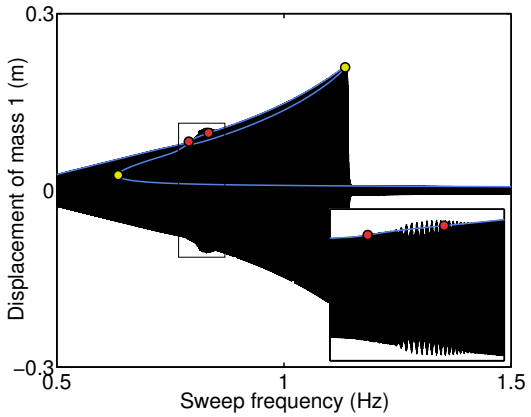

FIGURE 6: Response at mass 1 of the 2-DOF system to base, swept-sine (in black) and stepped-sine (in blue) excitations of 8 *mm* amplitude. Limit-point and Neimark-Sacker bifurcations on the stepped-sine response are depicted through yellow and red circles, respectively.

In order to gain further insights into the frequency jump revealed in Fig. 5, the response of the system to stepped-sine base excitations of 5, 6, 7 and 8 *mm* are plotted in Fig. 7 (a – d). Similarly to Fig. 6, LP and NS bifurcations are highlighted using yellow and red circles, respectively. The frequency-amplitude evolution of NNM 1 is also represented as a blue curve. A first key observation is the existence of an isola at 6 *mm* in Fig. 7 (b), lying outside the main branch [1], contrary to Fig. 7 (a) at 5 *mm* which only features a primary frequency response with two LP bifurcations. This observation agrees with the energy balance graph in Fig. 4 (b), which bounds the existence of multiple resonance locations associated with NNM 1 to a minimum forcing amplitude of 5.2 *mm*. Note that the isola in Fig. 7 (b) was computed by initialising the continuation algorithm using the resonance conditions predicted in Fig. 4 (b) for a base displacement of 6 *mm*. One also remarks the detection of two NS bifurcations on the isolated branch.

Increasing the forcing amplitude to 7 *mm* enlarges the domain of existence of the isola. The two resonance points on the isola correspond to frequencies of 0.80 and 1.08 *Hz*, as accurately predicted by the two upper dots in Fig. 4 (b). Increasing the forcing further to 8 *mm* finally leads to the merging of the primary and isolated solutions in the close vicinity of the 3:1 internal resonance visible in the NNM. Two close-ups of the merging region, including stability information, are provided in

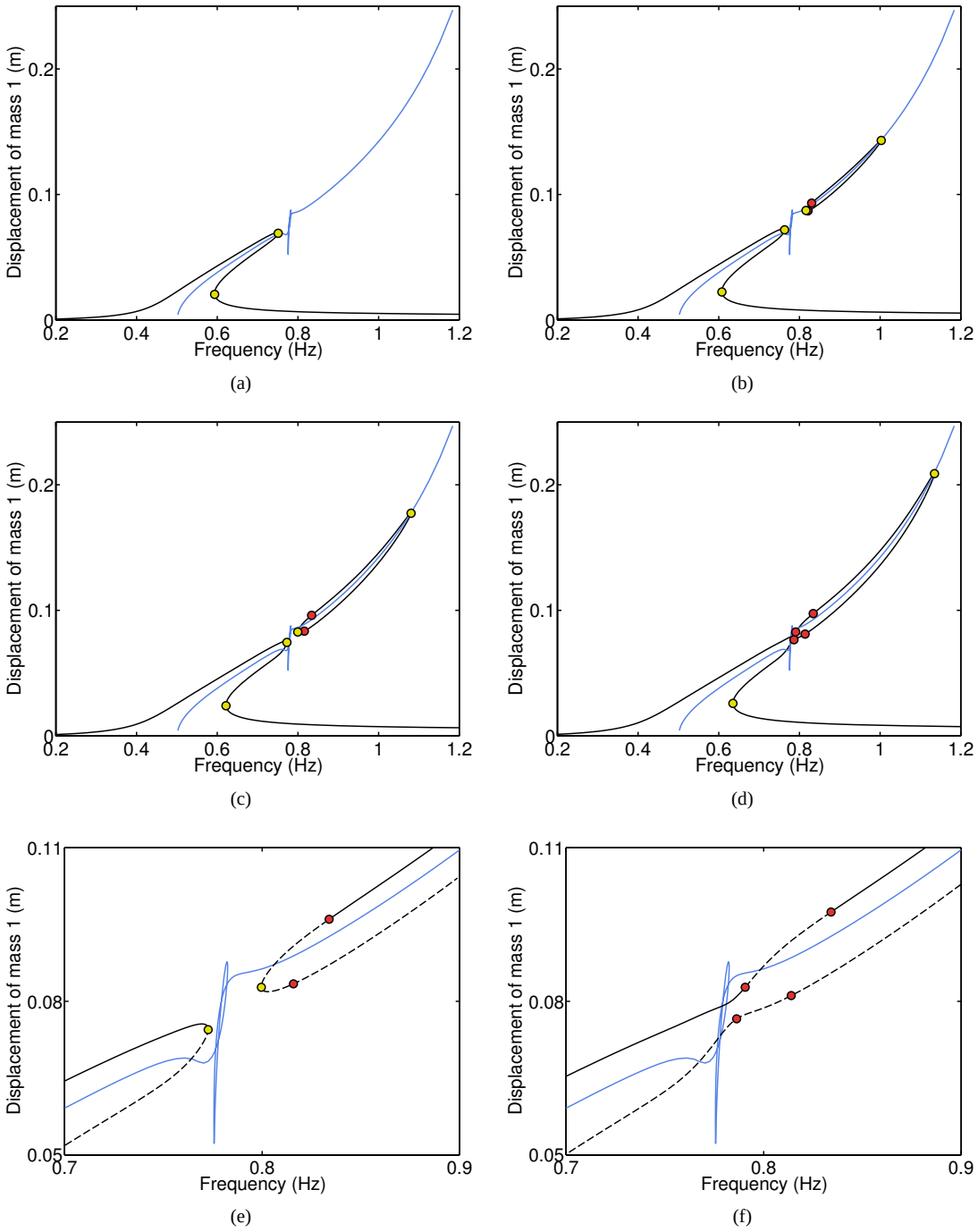

FIGURE 7: Response at mass 1 of the 2-DOF system to a base, stepped-sine excitation (in black) superposed on the first NNM amplitude-frequency curve of the system (in blue). Limit-point and Neimark-Sacker bifurcations on the response branches are depicted through yellow and red circles, respectively. (a – d) Base amplitude displacements of 5, 6, 7 and 8 *mm*. (e – f) Close-ups of the merging region in the 7 and 8 *mm* cases. In (e – f), stable and unstable periodic solutions are depicted using solid and dashed lines, respectively.

Fig. 7 (e – f) in the 7 and 8 mm cases. One notices that the merging occurs through the annihilation of two LP bifurcations. It is also seen that the quasiperiodic regime of motion analysed in Fig. 6 is generated by NS bifurcations originally located on the isola. In summary, the possibility for multiple resonance points evidenced in Fig. 4 (b), and originating in a α-loop internal resonance of NNM 1 in Fig. 4 (a), translates into an isolated response curve in the forced behaviour of the system. For a sufficiently large forcing amplitude, the main resonance branch and the isola may merge, modifying substantially the apparent resonance frequency and amplitude observed in sine-sweep testing.

3.4 Tracking of the limit-point bifurcations of the nonlinear forced response

LP bifurcations play an important role in the dynamics of isolas, as they dictate their domain of existence, including their onset and merging with the main forced response branch. The evolution of the LP bifurcations of the first resonance peak according to variations of various system parameters is analysed in this section using a tracking algorithm based on the harmonic balance method [16]. This algorithm employs in this study Fourier series truncated to nine harmonic components to approximate the solution of Eq. (2). The LP bifurcation curve is represented in the frequency-base displacement amplitude parameter space in Fig. 8 (a). Frequency responses to stepped-sine excitations of 5, 6, 7 and 8 *mm* are also plotted in black with LP bifurcations marked in yellow, and isolas are highlighted in red.

A convenient projection of the tracking curve is realised in Fig. 8 (b) in the frequency-base displacement amplitude plane (in black). The turning point in this figure, marked with a diamond, precisely locates the creation of the isolated solution at 0.876 *Hz* for a base displacement of 5.17 *mm*. The corresponding values inferred from the energy balance curve reproduced in blue in Fig. 8 (b), *i.e.* 0.881 *Hz* and 5.22 *mm*, are found to be in excellent agreement, which is a remarkable result given the importance of damping in the system. This confirms the great practicality of Eq. (4) to anticipate the existence of isolas based on the undamped system behaviour. The square marker in Fig. 8 (b) finally points out the location of the merging phenomenon at 7.72 *mm*, a value matching with the behaviour observed in Fig. 7 (c – f).

The influence on the LP curve of two parameters of the nonlinear restoring force in Eq. (2), namely λ and l, is examined in Fig. 8 (c – d). Positive and negative variations of 5 and 10 % are considered in the two graphs. Note that the prestress ratio λ has a maximum value of 1, which corresponds to no prestress, and so no linear stiffness term associated with the transverse springs. Fig. 8 (c) shows that increasing λ delays the onset and the merging of the isola to higher forcing magnitudes. The two extreme cases $\lambda = 0.81$ and $\lambda = 0.99$ are interesting. In the former in dashed blue, the LP curve monotonically increases, preventing the existence of isolated solutions. In the latter in dashed red, an isola is created at 6.72 *mm*, and merges at 16 *mm*, leading to a dramatic jump of the response amplitude from 0.10 *m* to 0.43 *m*. The parameter l impacts less importantly the LP curve, as depicted in Fig. 8 (d). Similarly to λ, increasing l delays the isola, but causes no significant modification of the response jump when merging.

Finally, Fig. 8 (e) analyses the modification of the LP curve according to variations of the stiffness k_2 of the linear spring connecting the two masses in Fig. 1. Positive and negative variations of 10 and 20 % are herein studied. Varying k_2 modifies the nominal ratio of 4.64 between the linear frequencies of the system, and so the location of the 3:1 internal resonance in the FEP of NNM 1. This results in Fig. 8 (e) not only in a delay of the isola for increasing k_2 values, similarly to previous cases, but also in an increase of the final response amplitude reached after merging. Practically speaking, the possibility to tune the parameter k_2 is attractive, as it alters the behaviour of the isola, without affecting the nonlinearity in the system.

3.5 Global analysis of periodic solutions: basins of attraction

An isolated response curve was shown in Fig. 5 to lead to an unexpectedly great level of response as it merges with the primary resonance peak. Another risk associated with isolas, when detached as in Fig. 7 (b – c), is the possibility to turn a low-amplitude oscillation on the main response branch to a high-amplitude oscillation on the isola by perturbing the system. A global analysis of periodic solutions via basins of attraction is performed in this section to determine the probability of such a perturbation to drive the system to the isolated solution branch.

Basins of attraction are plotted in Fig. 9 for base displacements of 6 and 7 *mm* (in the first and second column, respectively) and frequencies of 0.85, 0.9 and 0.95 *Hz* (in the first, second and third row, respectively). They were calculated through direct time integration assuming random initial conditions for mass 1 and zero initial conditions for mass 2. Grey and white regions correspond to stable periodic oscillations on the isola and on the main response branch, respectively. All six graphs prove that there exists a non-negligible probability to realise a periodic motion on the isola by adequately perturbing the system. An increase in forcing frequency at constant amplitude is also seen to translate into a modification of the attraction region of the isola, but not necessarily to a diminution of its size. By contrast, this region is found to shrink as the excitation amplitude decreases.

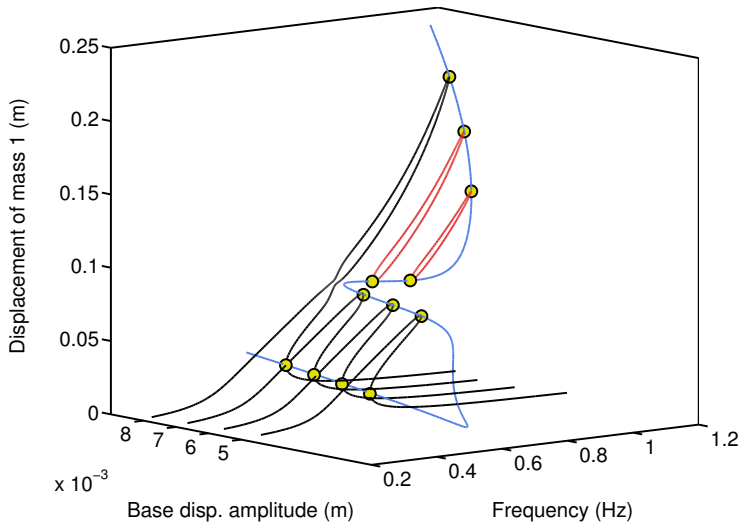

(a)

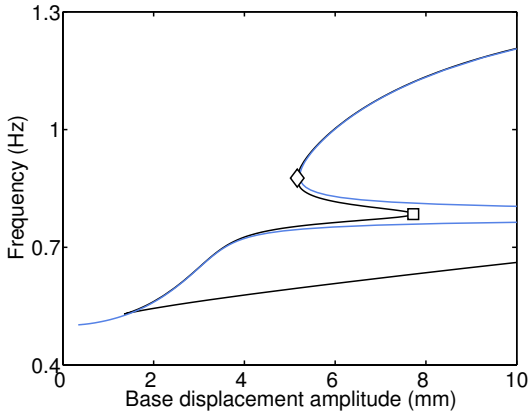

(b)

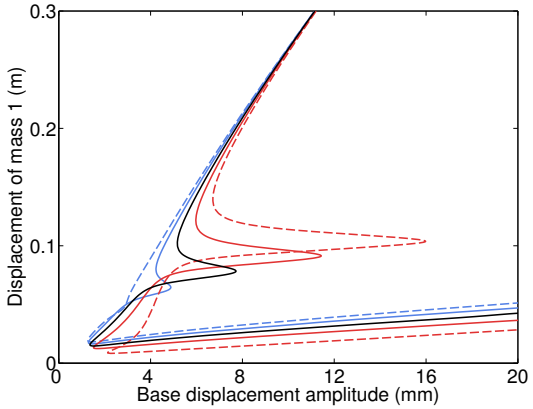

(c) $\lambda = 0.81$ (dashed blue); $\lambda = 0.855$ (solid blue); $\lambda = 0.9$ (black); $\lambda = 0.945$ (solid red); $\lambda = 0.99$ (dashed red).

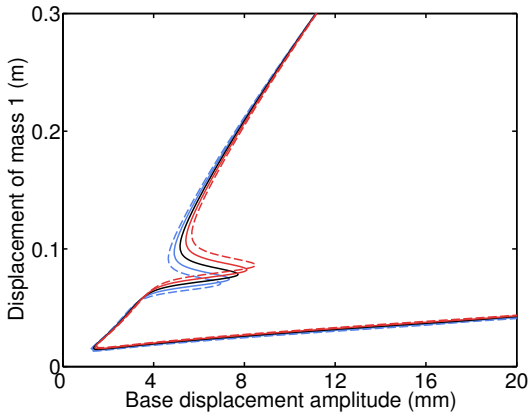

(d) $l = 0.09$ (dashed blue); $l = 0.095$ (solid blue); $l = 0.1$ (black); $l = 0.105$ (solid red); $l = 0.11$ (dashed red).

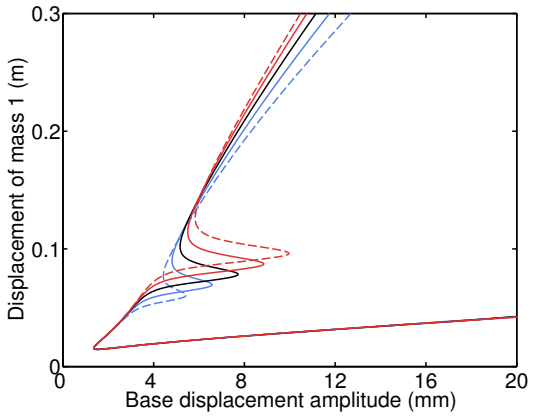

(e) $k_2 = 28$ (dashed blue); $k_2 = 31.5$ (solid blue); $k_2 = 35$ (black); $k_2 = 38.5$ (solid red); $k_2 = 42$ (dashed red).

FIGURE 8: (a) Tracking of the limit-point (LP) bifurcations of the 2-DOF system in the frequency-base displacement amplitude parameter space (in blue) superposed on frequency responses to stepped-sine excitations of 5, 6, 7 and 8 *mm* (in black). LP bifurcations on the frequency response curves are depicted through yellow circles, and isolas are highlighted in red. (b) Projection of the LP curve in the frequency-base displacement amplitude plane (in black) and energy balance curve of Fig. 4 (b) (in blue). (c – e) Evolution of the LP curve according to variations of λ, l and k_2, respectively.

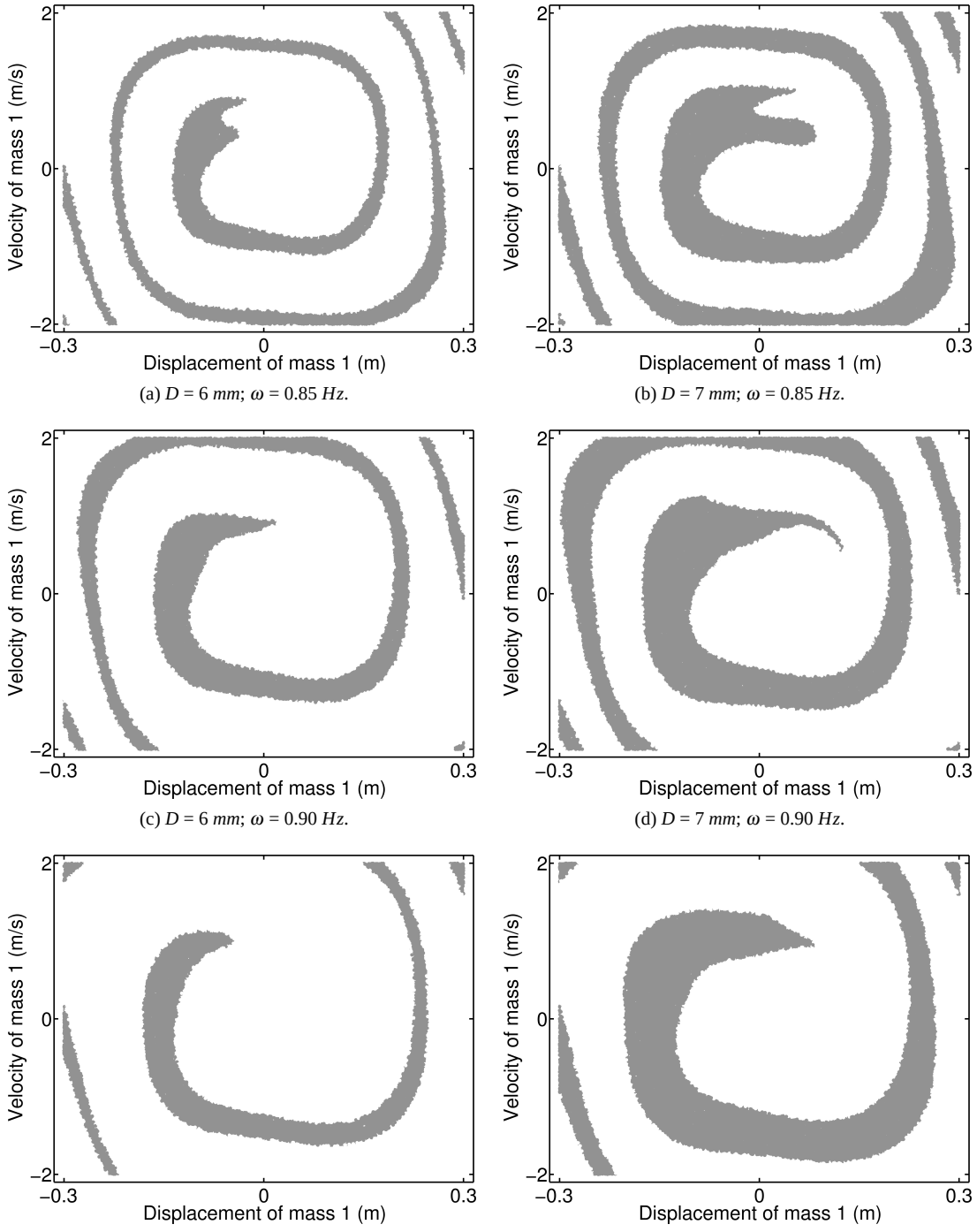

(a) $D = 6\ mm$; $\omega = 0.85\ Hz$.

(b) $D = 7\ mm$; $\omega = 0.85\ Hz$.

(c) $D = 6\ mm$; $\omega = 0.90\ Hz$.

(d) $D = 7\ mm$; $\omega = 0.90\ Hz$.

(e) $D = 6\ mm$; $\omega = 0.95\ Hz$.

(f) $D = 7\ mm$; $\omega = 0.95\ Hz$.

FIGURE 9: Basins of attraction of the 2-DOF system calculated assuming random initial conditions for mass 1 and zero initial conditions for mass 2. Grey and white regions correspond to stable periodic solutions on the isola and on the main response branch, respectively. Base displacement amplitudes and frequencies are given in the inset captions.

4 CONCLUSIONS

The objective of this paper was to investigate a series of intrinsic features of isolated response curves, or *isolas*, in a two-degree-of-freedom nonlinear system. Two conceptual tools, namely nonlinear normal modes and an energy balance criterion, were first utilised to relate modal interactions in the undamped, unforced system response and the creation of isolas. Limit-point bifurcations in the forced response were also analysed in detail since they govern their domain of existence. Moreover, it was shown that isolated solutions, as they merge with the main response branch through the annihilation of limit points, may impressively modify the resonance location. Finally, a global analysis was carried out to assess the practical existence of isolas.

Several dynamic features highlighted in the paper were too rapidly discussed for the sake of conciseness, and would hence deserve further investigation in future works. For instance, a more complete understanding of the quasi-periodic oscillations observed in Section 3.3 would be meaningful. Secondly, an extensive analysis of basins of attraction along the observed isolas, including in quasi-periodic regime of motion, would provide deeper insights. The possibility to create a 5:1 isolated solution in the system dynamics should also be examined, together with its potential interaction with the studied 3:1 isola. A final research prospect is the realisation of the mechanical system of interest in this paper, and the experimental characterisation of isolated response curves.

ACKNOWLEDGEMENTS

The author J.P. Noël is a Postdoctoral Researcher of the *Fonds de la Recherche Scientifique FNRS* which is gratefully acknowledged. The authors T. Detroux, L. Masset and G. Kerschen would also like to acknowledge the financial support of the European Union (ERC Starting Grant NoVib 307265).

REFERENCES

[1] Gatti, G., Brennan, M., and Kovacic, I., 2010. "On the interactions of the responses at the resonance frequencies of a nonlinear two degrees-of-freedom system". *Physica D,* ***239***, pp. 591–599.

[2] Duan, C., and Singh, R., 2008. "Isolated sub-harmonic resonance branch in the frequency response of an oscillator with slight asymmetry in the clearance". *Journal of Sound and Vibration,* ***314***, pp. 12–18.

[3] Alexander, N., and Schilder, F., 2009. "Exploring the performance of a nonlinear tuned mass damper". *Journal of Sound and Vibration,* ***319***, pp. 445–462.

[4] Murphy, K., Bayly, P., Virgin, L., and Gottwald, J., 1994. "Measuring the stability of periodic attractors using perturbation-induced transients: Application to two nonlinear oscillators". *Journal of Sound and Vibration,* ***172***(1), pp. 85–102.

[5] Virgin, L., 2000. *Introduction to Experimental Nonlinear Dynamics: A Case Study in Mechanical Vibration*. Cambridge University Press, Cambridge, United Kingdom.

[6] Kuether, R., Renson, L., Detroux, T., Grappasonni, C., Kerschen, G., and Allen, M., 2015. "Nonlinear normal modes, modal interactions and isolated resonance curves". *Journal of Sound and Vibration (in review)*.

[7] Rosenberg, R., 1962. "The normal modes of nonlinear n-degree-of-freedom systems". *Journal of Applied Mechanics,* ***29***, pp. 7–14.

[8] Rosenberg, R., 1966. "On nonlinear vibrations of systems with many degrees of freedom". *Advances in Applied Mechanics,* ***9***, pp. 217–240.

[9] Shaw, S., and Pierre, C., 1993. "Normal modes for nonlinear vibratory systems". *Journal of Sound and Vibration,* ***164***(1), pp. 85–124.

[10] Kerschen, G., Peeters, M., Golinval, J., and Vakakis, A., 2009. "Nonlinear normal modes. Part I: A useful framework for the structural dynamicist". *Mechanical Systems and Signal Processing,* ***23***(1), pp. 170–194.

[11] Peeters, M., Viguié, R., Sérandour, G., Kerschen, G., and Golinval, J., 2009. "Nonlinear normal modes. Part II: Toward a practical computation using numerical continuation techniques". *Mechanical Systems and Signal Processing,* ***23***(1), pp. 195–216.

[12] Peeters, M., Kerschen, G., and Golinval, J., 2011. "Dynamic testing of nonlinear vibrating structures using nonlinear normal modes". *Journal of Sound and Vibration,* ***330***, pp. 486–509.

[13] Peeters, M., Kerschen, G., and Golinval, J., 2011. "Modal testing of nonlinear vibrating structures based on nonlinear normal modes: Experimental demonstration". *Mechanical Systems and Signal Processing,* ***25***, pp. 1227–1247.

[14] Detroux, T., Renson, L., and Kerschen, G., 2014. "The harmonic balance method for advanced analysis and design of nonlinear mechanical systems". In Proceedings of the 32nd International Modal Analysis Conference (IMAC).

[15] Seydel, R., 2010. *Practical Bifurcation and Stability Analysis*. Springer, New-York, NY.

[16] Detroux, T., Renson, L., Masset, L., and Kerschen, G., 2015. "The harmonic balance method for bifurcation analysis of nonlinear mechanical systems". In Proceedings of the 33rd International Modal Analysis Conference (IMAC).